NeuroImage xxx (2011) xxx–xxx

Contents lists available at ScienceDirect

NeuroImage

journal homepage: www.elsevier.com/locate/ynimg

Heightened interactions between a key default-mode region and a key task-positive region are linked to suboptimal current performance but to enhanced future performance

Jérôme Prado [a,*], Daniel H. Weissman [b,*]

[a] Department of Communication Sciences and Disorders, Northwestern University, Evanston, IL 60208, United States
[b] Department of Psychology, University of Michigan, Ann Arbor, MI, 48109, United States

ARTICLE INFO

Article history:
Received 7 January 2011
Revised 9 March 2011
Accepted 17 March 2011
Available online xxxx

Keywords:
fMRI
Selective attention
Response time
Posterior cingulate cortex
Dorsolateral prefrontal cortex
Functional connectivity

ABSTRACT

According to the default-mode interference hypothesis, suboptimal performance in tasks requiring selective attention occurs when off-task processing (e.g., mind wandering) supported by default-mode regions interferes with on-task processing (e.g., attention) enabled by task-positive regions. In the present functional MRI study, we therefore investigated whether suboptimal performance in a selective attention task was linked to heightened interactions between a key default-mode region (the posterior cingulate cortex; PCC) and a key task-positive region (the left dorsolateral prefrontal cortex; DLPFC). We also investigated whether heightened interactions between the PCC and the left DLPFC were linked to enhanced future performance, consistent with prior data suggesting that such interactions index adaptive changes to the cognitive system. In line with both of these predictions, increases of current-trial functional connectivity between the PCC and the left DLPFC were linked to increases of response time in the current trial (i.e., suboptimal performance), but to decreases of response time in the next trial (i.e., enhanced performance). This double dissociation provides novel support for the default-mode interference hypothesis. Moreover, it suggests the possibility that, in at least some cases, default-mode interference indexes processes that optimize future performance.

Distinct brain regions are thought to support on- and off-task processing in attentional tasks. Regions in which activity increases when experimental stimuli are presented are thought to support on-task processing, such as voluntarily directing attention to relevant stimuli and locations in the environment and selecting an appropriate response (Posner and Petersen, 1990; Miller, 2000; Corbetta and Shulman, 2002). These so-called "task-positive" regions include the dorsolateral prefrontal cortex (DLPFC), the dorsal anterior cingulate cortex (ACC), the posterior parietal cortex (PPC), and the frontal eye fields (FEF). Regions in which activity decreases when experimental stimuli are presented are thought to support off-task processing (Raichle et al., 2001), such as self-referential thought (Gusnard et al., 2001) and mind wandering (Mason et al., 2007; Christoff et al., 2009). These so-called "task-negative" (or "default-mode") regions include the posterior cingulate cortex (PCC), the ventral medial prefrontal cortex (ventral mPFC), and both lateral and medial regions of the parietal cortex.

A number of findings indicate that suboptimal performance in selective attention tasks is associated with failing to deactivate default-mode regions. First, in healthy adults, both errors (Polli et al., 2005; Eichele et al., 2008) and relatively long response times (Weissman et al., 2006) are linked to heightened activity in default-mode regions. Second, a failure to fully deactivate default-mode regions has also been observed in populations who typically exhibit impaired performance on selective attention tasks, such as the elderly (Lustig et al., 2003) and patients with Alzheimer's disease (Sperling et al., 2009). These findings are consistent with the *default-mode interference hypothesis*: when off-task processing supported by default-mode regions is not effectively suppressed, it interferes with performance by disrupting on-task processing enabled by task-positive regions (Sonuga-Barke and Castellanos, 2007).

One way that such interference could occur is via increased communication, or *functional connectivity*, between default-mode and task-positive regions. Consistent with this possibility, resting-state activity in task-positive and default-mode regions that is negatively correlated in healthy adults (Fox et al., 2005) is less negatively correlated (possibly reflecting increased functional connectivity) in (a) individuals who exhibit symptoms of attention-deficit and hyperactivity disorder (ADHD) (Castellanos et al., 2008) and (b) healthy adults who exhibit relatively high response time variability during the performance of selective attention tasks (Kelly et al., 2008). However, such findings do not definitively link suboptimal performance to increased functional connectivity between default-mode and task-positive regions. First, the reduced

* Corresponding authors.
E-mail addresses: jerome-prado@northwestern.edu (J. Prado), danweiss@umich.edu (D.H. Weissman).

1053-8119/$ – see front matter © 2011 Elsevier Inc. All rights reserved.
doi:10.1016/j.neuroimage.2011.03.048

negative correlation between default-mode and task-positive regions in individuals who exhibit symptoms of ADHD was not correlated with a measure of suboptimal performance. Second, although heightened RT variability is a measure of suboptimal performance (Stuss et al., 2003), it may reflect periodic improvements in performance (e.g., decreases of RT) as well as the "periodic declines in performance" (e.g., increases of RT) that are posited to characterize default-mode interference (Sonuga-Barke and Castellanos, 2007). Thus, little evidence directly supports the view that default-mode interference is mediated by increased communication between default-mode and task-positive regions.

Adding to this uncertainty, other research suggests that increases of functional connectivity between default-mode and task-positive regions may underlie adaptive changes that enhance future performance. First, an increase of activity in the PCC, a key default-mode region (Buckner et al., 2008), predicts that a person will solve an upcoming problem through a flash of insight as compared to a more analytical approach (Kounios et al., 2006; Subramaniam et al., 2009). Second, when an anticipated reward is not received in a gambling task, increased firing rates in the PCC predict that a monkey will choose a potentially more rewarding option in the next trial (Hayden et al., 2008). These relationships between PCC activity and decision-making may be mediated by interactions between the PCC and the DLPFC, a key task-positive region that is critical for decision-making (Wallis, 2007) and executive control (Miller and Cohen, 2001). Consistent with this possibility, the PCC and the DLPFC are sometimes co-activated during the performance of decision-making tasks (Heekeren et al., 2004, 2006). Moreover, it has been suggested that co-activation of the PCC and the DLPFC underlies creativity, problem-solving, and other processes that enhance future performance (Christoff et al., 2009). To our knowledge, however, no prior study has shown that increased functional connectivity between the PCC and the DLPFC is linked to better future performance.

Together, the findings above suggest a novel hypothesis: interactions between the PCC and the DLPFC are associated with suboptimal current performance, but with enhanced future performance. In the present functional MRI study, we investigated this hypothesis by relating trial-by-trial measures of functional connectivity between the PCC and the DLPFC to trial-by-trial measures of performance. We predicted that, during the performance of a selective attention task, increases of current-trial functional connectivity between these regions would be linked to increases of response time in the current trial (i.e., suboptimal performance), but to decreases of response time in the next trial (i.e., enhanced performance).

Materials and methods

Participants

Sixteen healthy adults participated in the study. All were right-handed and had normal hearing, normal or corrected-to-normal vision, and no history of neurological or psychiatric disorders. Each gave informed written consent before the experiment and was paid $20 per hour. Two participants were excluded due to excessive head movement (i.e., greater than 3 mm). Data from three participants were excluded due to unusable eye tracker recordings. Eleven participants were thus included in our final analyses (four men; age range, 18–23 years; mean age, 21 years). All experimental procedures were approved by the University of Michigan Biomedical and Health Sciences Institutional Review Board.

Task and procedure

Participants performed two selective attention tasks in separate runs (Fig. 1). In each trial of the visual selective attention task (three runs), they identified a centrally-presented visual letter ("X" or "O";

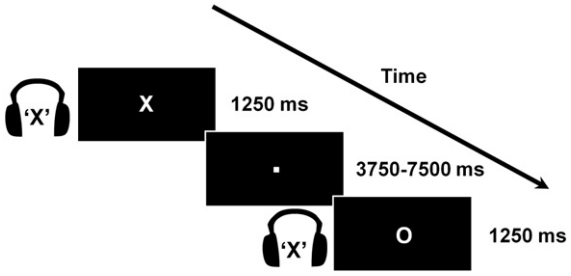

Fig. 1. Sample trials of the experimental task. In each trial (duration, 1250 ms), participants identified a relevant letter (i.e., "X" or "O"; duration, 350 ms) in one modality (e.g., visual) while ignoring an irrelevant letter (i.e., "X" or "O"; duration, 350 ms) in the other modality (e.g., auditory). The modality to which attention was directed (visual or auditory) varied across runs. Moreover, within each run, the auditory and visual letters were congruent in half the trials and incongruent in the other half. Variable periods of fixation separated trials (range: 3750–7500 ms, in units of 1250 ms).

1.72°×2.15° of visual angle; white against a black background; duration, 350 ms) while ignoring an auditory letter that was spoken in headphones ("X" or "O"; duration, 350 ms). The auditory letter was equally likely to be congruent or incongruent with the visual letter. The auditory selective attention task (three runs) made use of the same stimuli, but required participants to identify the auditory letter while ignoring the visual letter. The order of the visual and auditory selective attention tasks was counterbalanced across participants.

Variable periods of fixation were added after each trial (in units of the 1250 ms TR, ranging from 3750 ms to 7500 ms). The duration of these fixation periods was varied using a pseudo-exponential distribution that favored short inter-trial intervals (Ollinger et al., 2001). The experiment was divided into six runs of 80 trials each (40 congruent, 40 incongruent). The trials within each run were presented in a pseudo-random order such that each trial type was preceded equally often by every trial type in the design.

Half of the participants responded with their right index finger if the relevant letter was an X and with their right middle finger if the relevant letter was an O; this mapping was reversed in the other half of participants. Behavioral responses were recorded using an MR-compatible keypad placed below the right hand. Visual stimuli were generated using Presentation software (Neurobehavioral Systems, http://www.neurobs.com) and projected onto a translucent screen that was viewed by the participants through a mirror attached to the head-coil. Auditory stimuli were presented binaurally via GE MR-compatible, pneumatic sound transmission headphones. The same, clearly audible, volume level was used for all participants.

Eye tracking

Eye position and pupil size were recorded monocularly at 60 Hz during scanning by using an MR-compatible infrared video eye-tracker (NordicNeuroLab, Bergen, Norway). Before each run, the eye tracker was calibrated at a central position as well as at eight eccentric points. Analysis of eye movement data was performed off-line. For each trial, we analyzed the eye position traces from −100 to +400 ms post-stimulus onset. Trials in which subjects broke fixation were detected by calculating the derivative of the horizontal eye-position trace, i.e., saccade velocity. Trials in which subjects blinked were identified by measuring pupil size. When either saccade velocity exceeded 30°/s or pupil size equaled zero on a given trial, both this trial and the one immediately preceding it were excluded from further analysis (Macaluso et al., 2002). For two of the eleven participants who were included in the final analyses, one run was excluded from the functional MRI analyses because more than 30% of the trials were rejected due to eye movements.

Please cite this article as: Prado, J., Weissman, D.H., Heightened interactions between a key default-mode region and a key task-positive region are linked to suboptimal current performance..., NeuroImage (2011), doi:10.1016/j.neuroimage.2011.03.048

Imaging procedures

Images were collected using a 3-T GE Signa scanner (General Electric, Milwaukee, WI) equipped with a standard quadrature head coil. The blood oxygenation level dependent (BOLD) signal was measured with a reverse spiral imaging sequence (repetition time [TR] = 1250 ms, echo time [TE] = 30 ms). Twenty-seven contiguous axial slices (4.50-mm thick, field of view, 22 cm; in-plane resolution, 3.44 × 3.44 mm) were acquired per functional image. In each run, we collected 326 functional images. The first six images contained no trials and were discarded to allow for T1 equilibration effects.

Following functional image acquisition, a 3D spoiled gradient echo (SPGR), high-resolution, T1-weighted anatomical image was collected for each subject (TR = 10.5 ms, TE = 3.4 ms, FOV = 24 mm, flip angle = 25°, slice thickness = 1.5 mm).

Behavioral data analysis

We conducted two analyses of the behavioral data. First, the mean RT and mean error rate for each trial type were calculated separately in each participant and submitted to two random-effects analyses of variance (ANOVAs). Second, for each participant, we calculated the trial-by-trial correlation between current-trial RT and next-trial RT. Each participant-specific correlation was then converted to a z-value using Fisher's r to z transformation [0.5 × ln ((1 + r)/(1 − r))] so that we could test whether the mean correlation across participants differed from zero.

Functional MRI data analysis

A number of preprocessing steps were performed on the functional MRI data before trial-related activity was estimated. First, physiologic fluctuations were corrected using waveforms of respiration and cardiac cycles that were collected while participants performed the task in the scanner (Hu et al., 1995). Second, using SPM5 software (Wellcome Department of Cognitive Neurology, London, UK, http://www.fil.ion.ucl.ac.uk), the functional images were corrected for slice acquisition delays, spatially realigned to the first image of the first run to correct for head movements, normalized to the Montreal Neurological Institute (MNI) template (normalized voxel size, 3.45 × 3.45 × 4.5 mm), and spatially smoothed with an isotropic Gaussian filter (8-mm full width at half maximum).

Event-related regression analyses (conducted separately in each participant) were performed using a version of the general linear model in which the BOLD signal in each trial is modeled with a standard hemodynamic response function (Josephs et al., 1997). In each run, correct trials with RTs more than three standard deviations from the mean of their corresponding trial type (i.e., outliers) were excluded from behavioral and functional MRI analyses (2.0% of all trials). Errors (4.6% of trials) were also excluded from the analysis. All other correct trials were sorted by trial type (congruent, incongruent), such that separate regressors could be used to model average activity in congruent and incongruent trials.

We previously established that the amplitude of the stimulus-evoked BOLD response varies with trial-by-trial measures of RT in a predominantly linear fashion, both when a canonical hemodynamic response shape is assumed (Prado et al., 2011) and when it is not assumed (Chee et al., 2008). Given that some of our analyses assessed BOLD-RT relationships, however, it was important to verify that these relationships were also predominantly linear in the present study. Moreover, the absence of nonlinear effects would greatly simplify the process of quantifying BOLD-RT relationships. For these reasons, we used a polynomial regression approach to investigate whether the BOLD signal varied with RT in a predominantly linear fashion or whether it also varied with higher-order components of RT (i.e., quadratic, cubic, and quartic). In particular, for each voxel the brain response (y) was modeled by a general linear model of the following form:

$$y = \alpha_0 + \alpha_1(RT - \overline{RT}) + \alpha_2(RT - \overline{RT})^2 + \alpha_3(RT - \overline{RT})^3 + \alpha_4(RT - \overline{RT})^4 + \beta_0 + \varepsilon.$$

In this equation, the coefficient α_0 models the average response to each trial type (independent of RT) and the coefficients α_1, α_2, α_3 and α_4, respectively, model the linear (first-order), quadratic (second-order), cubic (third-order) and quartic (fourth-order) contribution of RT to the average hemodynamic response for each trial type. β_0 is the y-intercept term (a column of ones), and ε represents the residual error term after each component has been fitted to the data. Following Weissman et al. (2006) and Chee et al. (2008), the RT for each trial was mean-centered by subtracting the mean RT (i.e., $\overline{RT}$) for all correct trials of the corresponding trial type (i.e., congruent or incongruent) in the same functional run. The parameter estimate for the linear term was therefore calculated in units of *change in parameter estimate per second of increased RT*.

Regressors of no interest reflecting head motion were also included in the model. Moreover, the time series data from each run was high-pass filtered (1/128 Hz), and serial correlations were corrected using an autoregressive AR(1) model. Finally, random effects analyses on the beta values from each participant were used to account for between-participants variance and to ensure that any findings concerning stimulus-evoked activity would generalize to the population.

Functional connectivity analyses

We tested our hypotheses about functional connectivity using psychophysiological interaction (PPI) analyses (Friston et al., 1997; Gitelman et al., 2003). Such analyses assess whether interactions between brain regions vary with an experimental parameter. More specifically, they identify brain regions whose activity varies more or less strongly with activity in a seed region across the different levels of a psychological factor (Gitelman et al., 2003). Our analyses determined whether functional connectivity changed as a function of RT, trial type (congruent, incongruent), or with an interaction between these factors. To conduct these analyses, we extended the standard PPI analysis implemented in SPM5 to include multiple psychological factors and their interactions within the same multiple regression model (but different PPI analyses were used to investigate how functional connectivity varied with current-trial RT and next-trial RT to prevent the number of interaction terms from becoming too large).

PPI analyses in each participant were conducted in the following manner. To begin, we extracted the first eigenvariate time series from a sphere that was 6 mm in radius and centered on coordinates that were functionally defined in the present study. The regional time series from this sphere served as the first regressor in a PPI analysis (i.e., the "physiological" part of the PPI). Next, we entered the mean-centered RT and congruency value (1 or −1) in each trial, after they had each been convolved with a standard HRF, as the second and third regressors (the "psychological" parts of the PPI). Lastly, we entered regressors reflecting interactions between the physiological and psychological factors (i.e., the "interaction" parts of the PPI). To compute these interaction regressors, we first deconvolved the BOLD signal in the seed region by using a Bayesian estimation algorithm (Gitelman et al., 2003). We then multiplied various combinations of the RT, congruency, and deconvolved seed activity regressors (Gitelman et al., 2003) to produce four interaction terms: RT x Congruency, Seed x RT, Seed x Congruency, and Seed x RT x Congruency. These interaction terms were then convolved with a standard HRF.

Given that our main hypotheses concerned trial-by-trial relationships between functional connectivity and RT, it was important to establish whether these relationships were predominantly linear or

Please cite this article as: Prado, J., Weissman, D.H., Heightened interactions between a key default-mode region and a key task-positive region are linked to suboptimal current performance..., NeuroImage (2011), doi:10.1016/j.neuroimage.2011.03.048

whether functional connectivity also varied with higher-order components (i.e., quadratic, cubic, and quartic) of RT. Moreover, as in our analyses of BOLD-RT relationships, we reasoned that the absence of nonlinear effects would greatly simplify the process of characterizing how functional connectivity varied with RT. We therefore performed additional PPI analyses to determine whether functional connectivity varied with nonlinear components of RT. More specifically, for each voxel the brain response (y) was modeled by a general linear model of the following form:

$$y = \gamma_1 S_{PCC} + \gamma_2(RT-\overline{RT}) + \gamma_3(RT-\overline{RT})^2 + \gamma_4(RT-\overline{RT})^3 + \gamma_5(RT-\overline{RT})^4 + \gamma_6 S_{PCC}(RT-\overline{RT}) + \gamma_7 S_{PCC}(RT-\overline{RT})^2 + \gamma_8 S_{PCC}(RT-\overline{RT})^3 + \gamma_9 S_{PCC}(RT-\overline{RT})^4 + \delta_0 + \varepsilon.$$

In this equation, S_{PCC} represents the time course of the BOLD signal in the seed region (i.e., the "physiological" part of the PPI). Thus, γ1 represents the average functional connectivity with the PCC seed independent of RT. The coefficients γ2, γ3, γ4 and γ5, respectively, model the linear (first-order), quadratic (second-order), cubic (third-order) and quartic (fourth-order) contribution of RT to the average hemodynamic response for each trial type (i.e., the "psychological" parts of the PPI). The coefficients γ6, γ7, γ8 and γ9 represent the "interaction" terms of the PPI (i.e., the interactions between the physiological and psychological factors). That is, they model the linear (first-order), quadratic (second-order), cubic (third-order) and quartic (fourth-order) contribution of RT to functional connectivity with the PCC seed for each trial type (i.e., the "interaction" parts of the PPI). δ_0 is the y-intercept term (a column of ones), and ε represents the residual error term after each component has been fitted to the data.

As in our analyses of BOLD-RT relationships above, the RT for each trial was mean-centered by subtracting the mean RT for all correct trials of the corresponding trial type (i.e., congruent or incongruent) within the same functional run. The parameter estimate for the linear term was therefore calculated in units of *change in parameter estimate per second of increased RT*. Random effects analyses on the beta values from each participant were used to account for between-participants variance and to ensure that any findings concerning functional connectivity would generalize to the population.

Stepwise regression analysis

For activity and functional connectivity separately, we performed a serial forward stepwise regression analysis to assess the fit of each of the polynomial regressors to the data. In particular, starting with the zero-order component, we progressively added higher-order components (i.e., linear, quadratic, cubic, and quartic) to the regression equation. *F*-tests were used to determine which, if any, of these higher-order relationships between (1) activity and RT and (2) functional connectivity and RT improved the overall fit of the model.

Voxelwise analyses

Whole-brain analyses were conducted with a voxel height threshold of $p<0.005$ and a cluster extent of at least 24 contiguous voxels. These thresholds reduced the voxelwise probability of false positives to $p<0.05$ over the whole-brain, as determined by a Monte Carlo simulation (5000 iterations over the whole-brain) using the 'AlphaSim' program (http://www.afni.nimh.nih.gov/afni/docpdf/alphasim.pdf). All coordinates are reported in MNI space.

Region of interest analyses

Region of interest (ROI) analyses were conducted using the SPM toolbox Marsbar (http://www.marsbar.sourceforge.net/). ROIs included all voxels within a 6 mm radius of each coordinate of interest. For each participant, we calculated the average activity and functional connectivity associated with each trial type after averaging the fMRI signal across all voxels within that ROI. Unless otherwise noted, one-tailed p values were reported because most of our hypotheses were directional. P values less than 0.05 were considered to be significant.

Results

Overall behavior

A repeated-measures ANOVA with the factors task (visual, auditory) and congruency (congruent, incongruent) and mean RT as the dependent measure revealed two main effects and an interaction. First, replicating our prior findings from similar tasks (Weissman et al., 2004; Moore et al., 2009; Orr and Weissman, 2009), there was a main effect of congruency, $F(1,10)=4.82$, $p=0.013$, since mean RT was longer in incongruent (681 ms) than in congruent trials (652 ms). Second, and also replicating our prior findings, there was a main effect of task, $F(1,10)=11.45$, $p=0.007$, because mean RT was longer in the auditory task (697 ms) than in the visual task (624 ms). Third, there was an interaction between task and congruency, $F(1,10)=7.18$, $p=0.002$: the congruency effect was larger in the auditory task (64 ms; $t(10)=6.97$, $P=0.00002$) than in the visual task (19 ms; $t(10)=1.60$, $p=0.07$).

An analogous repeated-measures ANOVA with the factors task (visual, auditory) and congruency (congruent, incongruent) and mean error rate as the dependent measure revealed a main effect of congruency because error rates were higher in incongruent (5.4%) than in congruent trials (3.7%), $F(1,10)=8.02$, $p=0.018$. There was no main effect of task, $F(1,10)=0.16$, $p=0.69$, and no interaction between task and congruency $F(1,10)=0.03$, $p=0.86$.

Functional MRI

The PCC was deactivated during task performance

We chose a region of the PCC to serve as the seed region in the main functional connectivity analyses. To identify such a region, we capitalized on the fact that default-mode regions are deactivated during task performance. Specifically, we contrasted all stimuli to baseline in a voxelwise analysis. In the resulting statistical map, we then selected the voxel with the most negative t-value, $t(10)=-2.51$, $p=0.015$, indicating a deactivation, in a mask that included only the precuneus and the PCC (this mask was created using Pickatlas http://www.fmri.wfubmc.edu/download.htm). The PCC seed region was an ROI centered on this voxel ($x=-7$, $y=-41$, $z=40$; Fig. 2A).

The left DLPFC was activated during task performance

Our main hypothesis concerned whether functional connectivity between the PCC and the DLPFC varied with RT. We therefore wished to identify a ROI in the DLPFC without biasing the outcome of our functional connectivity analyses. To do so, we defined a ROI in the DLPFC whose activity (not functional connectivity) varied with RT. This ROI was centered on the peak activation in bilateral DLPFC in a voxelwise map depicting regions whose activity increased linearly with RT. More specifically, the peak coordinate of this activation was centered in Brodmann area 9 of the left DLPFC ($x=-41$, $y=38$, $z=27$).

Activity in the DLFPC ROI was as expected for a task-positive region. First, it rose above baseline during task performance ($t(10)=4.86$, $p=0.0003$). Second, it was greater in incongruent than in

Please cite this article as: Prado, J., Weissman, D.H., Heightened interactions between a key default-mode region and a key task-positive region are linked to suboptimal current performance..., NeuroImage (2011), doi:10.1016/j.neuroimage.2011.03.048

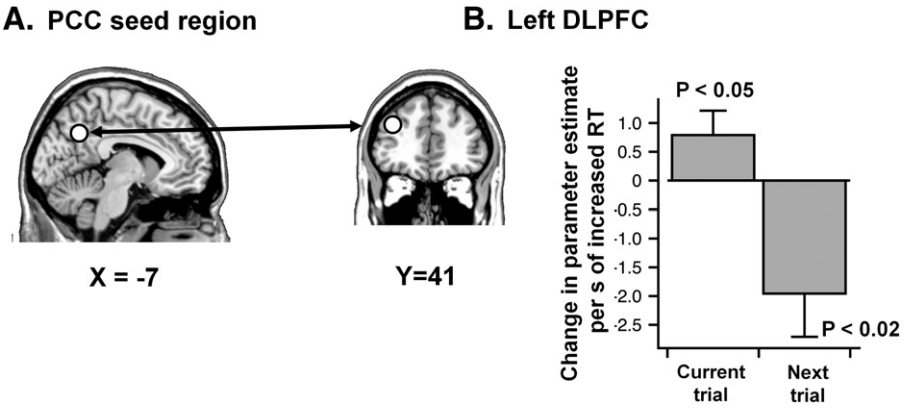

Fig. 2. RT-connectivity relationships involving the PCC seed region and the left DLPFC. (A) the seed region of PCC (x = −7, y = −41, z = 40; 6-mm radius) in the PPI analyses. (B) both slower current-trial RT and faster next-trial RT were linked to increased current-trial functional connectivity between the PCC and the left DLPFC. The PCC and the left DLPFC are each overlaid on a slice of the MNI-normalized anatomical brain.

congruent trials ($t(10) = 1.88$, $p = 0.04$) (Weissman et al., 2004; Orr and Weissman, 2009). Third, in line with prior results (Chee et al., 2008; Prado et al., 2011), polynomial and stepwise regression analyses (see Materials and methods) did not reveal nonlinear relationships between activity and current-trial RT or next-trial RT in this ROIs (all $p > 0.05$).

A double dissociation for current and future performance involving functional connectivity between the PCC and the left DLPFC

We hypothesized that trial-by-trial increases of functional connectivity between the PCC and the DLPFC would be associated with increases of RT in the current trial, but with decreases of RT in the next trial. To simplify the process of quantifying RT-connectivity relationships, we assumed an absence of nonlinear relationships between stimulus-evoked functional connectivity and RT. In line with this assumption, PPI and stepwise regression analyses (see Materials and Methods) did not reveal the presence of nonlinear relationships (i.e., quadratic, cubic, and quartic) involving functional connectivity between the PCC and the left DLPFC, either in the current trial or in the next trial (all $p > 0.05$).

Most important, we observed a double dissociation for current and future performance involving functional connectivity between the PCC and the left DLPFC. First, as predicted by the default-mode interference hypothesis, increases of current-trial functional connectivity between these regions were linearly related to *increases* of RT in the current trial, $t(10) = 2.18$, $p = 0.027$ (Fig. 2B, left side of plot). Second, as predicted by the view that interactions between the PCC and the left DLPFC enhance future performance, increases of current-trial functional connectivity between these regions were linearly related to *decreases* of RT in the next trial, $t(10) = 2.39$, $p = 0.019$ (Fig. 2B, right side of plot). Third, and indicating the presence of a double dissociation, increases of current-trial functional connectivity between the PCC and the left DLPFC were related to linear increases of RT more strongly in the current trial than in the next trial, $t(10) = 3.53$, $p = 0.003$. In sum, consistent with predictions our findings revealed a double dissociation for current and future performance involving functional connectivity between the PCC and the left DLPFC.

Control analyses

The RT-connectivity effects above are consistent with our hypothesis. However, it is important to show that similar effects do not occur regardless of the seed region that is chosen for the functional connectivity analysis. Thus, we performed control analyses in which a region of the left primary motor cortex (x = −47, y = −14, z = 54; BA 4; centered on the peak primary motor cortex activation in a contrast of all stimuli versus baseline) served as the seed region in our functional connectivity analyses.

These analyses verified that the RT-connectivity effects we observed were specific to the PCC seed region. First, one-tailed t-tests revealed that increases of current-trial functional connectivity between the primary motor cortex seed and the left DLPFC were not associated with increases of RT in the current trial ($t(10) = -0.82$, $p = 0.784$) or with decreases of RT in the next trial ($t(10) = 0.18$, $p = 0.43$). Second, indicating the absence of a double dissociation the RT-connectivity relationships above did not differ from one another ($t(10) = -0.25$, $p = 0.597$). Third, the double dissociation observed when the PCC served as the seed region was significantly larger than the (lack of a) double dissociation observed when the left primary motor cortex served as the seed region ($t(10) = 1.93$, $p = 0.03$). Thus, as expected, we did not observe a double dissociation for current and future performance involving functional connectivity between the left primary motor cortex and the left DLPFC.

Three additional findings ruled out the possibility that the opposing RT-connectivity relationships involving the PCC and the left DLPFC were simply driven by a negative correlation between current-trial RT and next-trial RT. First, if all RT-connectivity relationships in our task were driven by a negative relationship between current-trial RT and next-trial RT, then we should have seen exactly the same RT-connectivity relationships between the left primary motor cortex and the left DLPFC above as we did between the PCC and the left DLPFC. As described above, however, this result was not obtained. Second, random effects analyses revealed a small positive (not negative) correlation between current-trial RT and next-trial RT (average $r = 0.10$; $t(10) = 3.38$, $p < 0.007$). Third, an across-participants correlation revealed no significant relationship between the strength of this positive correlation and the degree to which increases of current-trial functional connectivity between the PCC and the left DLPFC were linked to decreases of RT in the next trial ($r = -0.18$, $p = 0.58$). In sum, the opposing RT-connectivity relationships (current trial versus next trial) involving the PCC and the left DLPFC were not driven by a negative correlation between current-trial RT and next-trial RT.

Discussion

In the present study, we investigated a novel hypothesis: heightened interactions between the PCC and the DLPFC are linked to suboptimal current performance, but to enhanced future performance. Consistent with this view, increases of current-trial functional connectivity between these regions were associated with increases of current-trial RT, but with decreases of next-trial RT. As described below, these findings provide novel support for the default-mode

Please cite this article as: Prado, J., Weissman, D.H., Heightened interactions between a key default-mode region and a key task-positive region are linked to suboptimal current performance..., NeuroImage (2011), doi:10.1016/j.neuroimage.2011.03.048

interference hypothesis (Sonuga-Barke and Castellanos, 2007; Castellanos et al., 2008; Kelly et al., 2008). They also extend recent work based on activity (not functional connectivity) analyses, which suggests that heightened interactions between default-mode and task-positive regions might serve to enhance future performance (Heekeren et al., 2004, 2006; Kounios et al., 2006; Hayden et al., 2008; Christoff et al., 2009; Subramaniam et al., 2009).

The default-mode interference hypothesis

According to the default-mode interference hypothesis, suboptimal performance in selective attention tasks occurs when off-task processing supported by default-mode regions interferes with on-task processing enabled by task-positive regions (Sonuga-Barke and Castellanos, 2007). We reasoned that one way that such interference could occur is via increased communication between default-mode and task-positive regions. Consistent with this view, we found that increases of RT in the current trial were linked to increases of current-trial functional connectivity between a key default-mode region (the PCC) and a key task-positive region (the left DLPFC). This result provides novel support for the default-mode interference hypothesis.

This result also answers an important question concerning whether default-mode interference is all-or-none or graded in nature (Sonuga-Barke and Castellanos, 2007). In an all-or-none scenario, default-mode regions disrupt processing in task-positive regions only when interactions between these regions reach a critical threshold. In a graded scenario, default-mode regions disrupt processing in task-positive regions more continuously, such that the level of disruption scales with the level of interaction. The present findings support the graded scenario by indicating the presence of linear RT-connectivity relationships between the PCC and the left DLPFC. Thus, in addition to theorizing about discrete on- and off-task states (Smallwood et al., 2008; Christoff et al., 2009), it may be fruitful to conceptualize default-mode interference along a continuum. Notably, this conceptualization is consistent with prior findings indicating that activity in default-mode regions is suppressed to varying (rather than constant) degrees during task performance (McKierman et al., 2003; Weissman et al., 2006).

How might heightened interactions between the PCC and the left DLPFC interfere with current performance? The left DLPFC has been implicated in a variety of resource-limited functions including those related to working memory (Miller and Cohen, 2001) and executive control (MacDonald et al., 2000). In theory, disrupting any of these functions could interfere with current performance. For example, utilizing working memory resources to maintain the contents of mind wandering episodes could decrease the resources that are available to maintain task goals, thereby leading to an increase of RT. Alternatively, RT slowing might vary with how actively the DLPFC is engaged in suppressing activity in the PCC, thereby leaving it with fewer resources to maintain task goals. Future studies will be needed to investigate these and other possible accounts. Whatever the outcome, the present findings provide novel support for the default-mode interference hypothesis.

Heightened interactions between the PCC and the left DLPFC predict enhanced future performance

The present findings are also consistent with recent work suggesting that heightened interactions between the PCC and the left DLPFC might be linked to enhanced future performance. Specifically, increases of current-trial functional connectivity between the PCC and the left DLPFC were linked to *decreases* of next-trial RT. At present, we can only speculate as to the nature of this effect. First, it may index an adaptive influence of the PCC on decision-making circuitry in the DLPFC, which aids future performance. This view fits with data indicating that increases of PCC activity predict upcoming flashes of insight (Kounios et al., 2006; Subramaniam et al., 2009) and changes in response strategy following reward-based feedback (Hayden et al., 2008). Second, it may index processes that retrieve task instructions (e.g., stimulus–response mappings) from memory when current performance declines, thereby aiding future performance. This possibility is in line with data indicating a role for the PCC in episodic memory retrieval (Andreasen et al., 1995; Duzel et al., 1999). Third, it may index processes that support mind wandering. This view fits with the suggestion that, although mind wandering undermines current performance (Christoff et al., 2009), it may serve to "organize what could not be organized during stimulus presentation, solve problems that require computation over long periods of time, and create effective plans governing behavior in the future" (Binder et al., 1999). Given these various possible explanations, additional studies will be needed to determine exactly how communication between the PCC and the left DLPFC enhances future performance. Regardless of the outcome, the effects we have observed indicate that interactions between these regions are linked to enhanced future performance.

A double dissociation for current and future performance involving functional connectivity between the PCC and the left DLPFC

To our knowledge, the present findings provide the first evidence of a double dissociation for current and future performance involving functional connectivity between a key default-mode region (the PCC) and a key task-positive region (the left DLPFC). As such, they serve to integrate two literatures that have proceeded somewhat independently: one that associates default-mode regions with suboptimal current performance (Castellanos et al., 2008; Kelly et al., 2008) and a second that suggests these regions may function to enhance future performance (Christoff et al., 2009; Kounios et al., 2006; Subramaniam et al., 2009). Moreover, the double dissociation that we observed may serve to constrain theories about how interactions between default-mode and task-positive regions influence goal-directed behavior. For example, it suggests that participants make adaptive changes to the cognitive system during off-task processing that draw resources away from current performance, but optimize future performance. Of importance, a double dissociation for current and future performance was not observed when our functional connectivity analyses employed the left primary motor cortex as the seed region. Thus, the dissociation that we observed was not a general phenomenon involving all brain regions that contributed to performance.

Clinical relevance

It has been proposed that suboptimal performance in individuals with ADHD reflects heightened levels of default-mode interference. However, previous studies have provided relatively indirect evidence to support this view. For example, relative to controls, individuals with ADHD exhibit reductions in the degree to which resting-state activity in default-mode and task-positive regions is negatively correlated (Castellanos et al., 2008). In contrast, the present findings directly link *RT slowing*, an objective measure of suboptimal performance, to heightened functional connectivity between a key default-mode region and a key task-positive region. Future studies might therefore investigate whether this effect is especially pronounced in individuals with ADHD.

Conclusions

The present findings make several important contributions to the literature. First, they provide novel support for the default-mode interference hypothesis. Second, they suggest that default-mode interference is continuous (rather than discrete) in nature. Third, they show that heightened interactions between a key default-mode

Please cite this article as: Prado, J., Weissman, D.H., Heightened interactions between a key default-mode region and a key task-positive region are linked to suboptimal current performance..., NeuroImage (2011), doi:10.1016/j.neuroimage.2011.03.048

region and a key task-positive region are linked to enhanced future performance. Fourth, they indicate a novel double dissociation for current and future performance that is based solely on RT-connectivity relationships between these regions. Future studies may shed additional light on the RT-connectivity relationships we have observed by investigating the cognitive processes they reflect and whether they are altered in clinical syndromes that are characterized by attentional impairments (e.g., ADHD).

Acknowledgments

This research was supported by startup funds provided to Daniel H. Weissman by the University of Michigan. We thank Keith Newnham for his assistance in collecting the fMRI data.

References

Andreasen, N.C., O'Leary, D.S., Cizadlo, T., Arndt, S., Rezai, K., Watkins, G.L., Ponto, L.L., Hichwa, R.D., 1995. Remembering the past: two facets of episodic memory explored with positron emission tomography. Am. J. Psychiatry 152, 1576–1585.

Binder, J.R., Frost, J.A., Hammeke, T.A., Bellgowan, P.S., Rao, S.M., Cox, R.W., 1999. Conceptual processing during the conscious resting state. A functional MRI study. J. Cogn. Neurosci. 11, 80–95.

Buckner, R.L., Andrews-Hanna, J.R., Schacter, D.L., 2008. The brain's default network: anatomy, function, and relevance to disease. Ann. N Y Acad. Sci. 1124, 1–38.

Castellanos, F.X., Margulies, D.S., Kelly, C., Uddin, L.Q., Ghaffari, M., Kirsch, A., Shaw, D., Shehzad, Z., Di Martino, A., Biswal, B., Sonuga-Barke, E.J., Rotrosen, J., Adler, L.A., Milham, M.P., 2008. Cingulate-precuneus interactions: a new locus of dysfunction in adult attention-deficit/hyperactivity disorder. Biol. Psychiatry 63, 332–337.

Chee, M.W., Tan, J.C., Zheng, H., Parimal, S., Weissman, D.H., Zagorodnov, V., Dinges, D.F., 2008. Lapsing during sleep deprivation is associated with distributed changes in brain activation. J. Neurosci. 28, 5519–5528.

Christoff, K., Gordon, A.M., Smallwood, J., Smith, R., Schooler, J.W., 2009. Experience sampling during fMRI reveals default network and executive system contributions to mind wandering. Proc. Natl Acad. Sci. U. S. A. 106, 8719–8724.

Corbetta, M., Shulman, G.L., 2002. Control of goal-directed and stimulus-driven attention in the brain. Nat. Rev. Neurosci. 3, 201–215.

Duzel, E., Cabeza, R., Picton, T.W., Yonelinas, A.P., Scheich, H., Heinze, H.J., Tulving, E., 1999. Task-related and item-related brain processes of memory retrieval. Proc. Natl Acad. Sci. U. S. A. 96, 1794–1799.

Eichele, T., Debener, S., Calhoun, V.D., Specht, K., Engell, A.K., Hugdahl, K., von Kramon, D.Y., Ullsberger, M., 2008. Prediction of human errors by maladaptive changes in event-related brain networks. Proc. Natl Acad. Sci. U. S. A. 105, 6173–6178.

Fox, M.D., Snyder, A.Z., Vincent, J.L., Corbetta, M., Van Essen, D.C., Raichle, M.E., 2005. The human brain is intrinsically organized into dynamic, anticorrelated functional networks. Proc. Natl Acad. Sci. U. S. A. 102, 9673–9678.

Friston, K.J., Bueschel, C., Fink, G.R., Morris, J., Rolls, E., Dolan, R.J., 1997. Psychophysiological and modulatory interactions in neuroimaging. NeuroImage 6, 218–229.

Gitelman, D.R., Penny, W.D., Ashburner, J., Friston, K.J., 2003. Modeling regional and psychophysiologic interactions in fMRI: the importance of hemodynamic deconvolution. NeuroImage 19, 200–207.

Gusnard, D.A., Akbudak, E., Shulman, G.L., Raichle, M.E., 2001. Medial prefrontal cortex and self-referential mental activity: relation to a default mode of brain function. Proc. Natl Acad. Sci. U. S. A. 98, 4259–4264.

Hayden, B.Y., Nair, A.C., McCoy, A.N., Platt, M.L., 2008. Posterior cingulate cortex mediates outcome-contingent allocation of behavior. Neuron 60, 19–25.

Heekeren, H.R., Marrett, S., Bandettini, P.A., Ungerleider, L.G., 2004. A general mechanism for perceptual decision-making in the human brain. Nature 431, 859–862.

Heekeren, H.R., Marrett, S., Ruff, D.A., Bandettini, P.A., Ungerleider, L.G., 2006. Involvement of human left dorsolateral prefrontal cortex in perceptual decision making is independent of response modality. Proc. Natl Acad. Sci. U. S. A. 103, 10023–10028.

Hu, X., Le, T.H., Parrish, T., Erhard, P., 1995. Retrospective estimation and correction of physiological fluctuation in functional MRI. Magn. Reson. Med. 34, 201–212.

Josephs, O., Turner, R., Friston, K., 1997. Event-related fMRI. Hum. Brain Mapp. 5, 1–7.

Kelly, A.M., Uddin, L.Q., Biswal, B.B., Castellanos, F.X., Milham, M.P., 2008. Competition between functiional brain networks mediates behavioral variability. NeuroImage 39, 527–537.

Kounios, J., Frymiare, J.L., Bowden, E.M., Fleck, J.I., Subramaniam, K., Parrish, T.B., Jung-Beeman, M., 2006. The prepared mind: neural activity prior to problem presentation predicts subsequent solution by sudden insight. Psychol. Sci. 17, 882–890.

Lustig, C., Snyder, A.Z., Bhakta, M., O'Brien, K.C., McAvoy, M., Raichle, M.E., Morris, J.C., Buckner, R.L., 2003. Functional deactivations: change with age and dementia of the Alzheimer type. Proc. Natl Acad. Sci. U. S. A. 100, 14504–14509.

Macaluso, E., Frith, C.D., Driver, J., 2002. Supramodal effects of covert spatial orienting triggered by visual or tactile events. J. Cogn. Neurosci. 14, 389–401.

MacDonald, A.W., Cohen, J.D., Stenger, V.A., Carter, C.S., 2000. Dissociating the role of the dorsolateral prefrontal and anterior cingulate cortex in cognitive control. Science 288, 1835–1838.

Mason, M.F., Norton, M.I., Van Horn, J.D., Wegner, D.M., Grafton, S.T., Macrae, C.N., 2007. Wandering minds: the default network and stimulus-independent thought. Science 19, 393–395.

McKierman, K.A., Kaufman, J.N., Kucera-Thompson, J., Binder, J.R., 2003. A parametric manipulation of factors affecting task-induced deactivation in functional neuroimaging. J. Cogn. Neurosci. 15, 394–408.

Miller, E.K., 2000. The prefrontal cortex and cognitive control. Nat. Rev. Neurosci. 1, 59–65.

Miller, E.K., Cohen, J.D., 2001. An integrative theory of prefrontal cortex function. Annu. Rev. Neurosci. 24, 167–202.

Moore, K.S., Porter, C.B., Weissman, D.H., 2009. Made you look! Irrelevant commands can hijack the attentional network. NeuroImage 46, 270–279.

Ollinger, J.M., Corbetta, M., Shulman, G.L., 2001. Separating processes within a trial in event-related functional MRI 13, 218–229.

Orr, J.M., Weissman, D.H., 2009. Anterior cingulate cortex makes 2 contributions to minimizing distraction. Cerebral Cortex. 19, 703–711.

Polli, F.E., Barton, J.J., Cain, M.S., Thakkar, K.N., Rauch, S.L., Manoach, D.S., 2005. Rostral and dorsal anterior cingulate cortex make dissociable contributions during antisaccade error commission. Proc. Natl Acad. Sci. U. S. A. 102, 15700–15705.

Posner, M.I., Petersen, S.E., 1990. The attention system of the human brain. Annu. Rev. Neurosci. 13, 25–42.

Prado, J., Carp, J., Weissman, D.H., 2011. Variations of response time in a selective attention task are linked to variations of functional connectivity in the attentional network. Neuroimage 54, 541–549.

Raichle, M.E., MacLeod, A.M., Snyder, A.Z., Powers, W.J., Gusnard, D.A., Shulman, G.L., 2001. A default mode of brain function. Proc. Natl Acad. Sci. U. S. A. 98, 676–682.

Smallwood, J., Beach, E., Schooler, J.W., Handy, T.C., 2008. Going AWOL in the brain: mind wandering reduces cortical analysis of external events. J. Cogn. Neurosci. 20, 458–469.

Sonuga-Barke, E.J., Castellanos, F.X., 2007. Spontaneous attentional fluctuations in impaired states and pathological conditions: a neurobiological hypothesis. Neurosci. Biobehav. Rev. 31, 977–986.

Sperling, R.A., Laviolette, P.S., O'Keefe, K., O'Brien, J., Rentz, D.M., Pihlajamaki, M., Marshall, G., Hyman, B.T., Selkoe, D.J., Hedden, T., Buckner, R.L., Becker, J.A., Johnson, K.A., 2009. Amyloid deposition is associated with impaired default network function in older persons without dementia. Neuron 63, 178–188.

Stuss, D.T., Murphy, K.J., Binns, M.A., Alexander, M.P., 2003. Staying on the job: the frontal lobes control individual performance variability. Brain 126, 2363–2380.

Subramaniam, K., Kounios, J., Parrish, T.B., Jung-Beeman, M., 2009. A brain mechanism for facilitation of insight by positive affect. J. Cogn. Neurosci. 21, 415–432.

Wallis, J.D., 2007. Neuronal mechanisms in prefrontal cortex underlying adaptive choice behavior. Ann N Y Acad Sci. 1121, 447–460.

Weissman, D.H., Warner, L.M., Woldorff, M.G., 2004. The neural mechanisms for minimizing cross-modal distraction. J. Neurosci. 24, 10941–10949.

Weissman, D.H., Roberts, K.C., Visscher, K.M., Woldorff, M.G., 2006. The neural bases of momentary lapses in attention. Nat. Neurosci. 9, 971–978.

Please cite this article as: Prado, J., Weissman, D.H., Heightened interactions between a key default-mode region and a key task-positive region are linked to suboptimal current performance..., NeuroImage (2011), doi:10.1016/j.neuroimage.2011.03.048